Max-Planck-Institut
für Meteorologie

REPORT No. 110

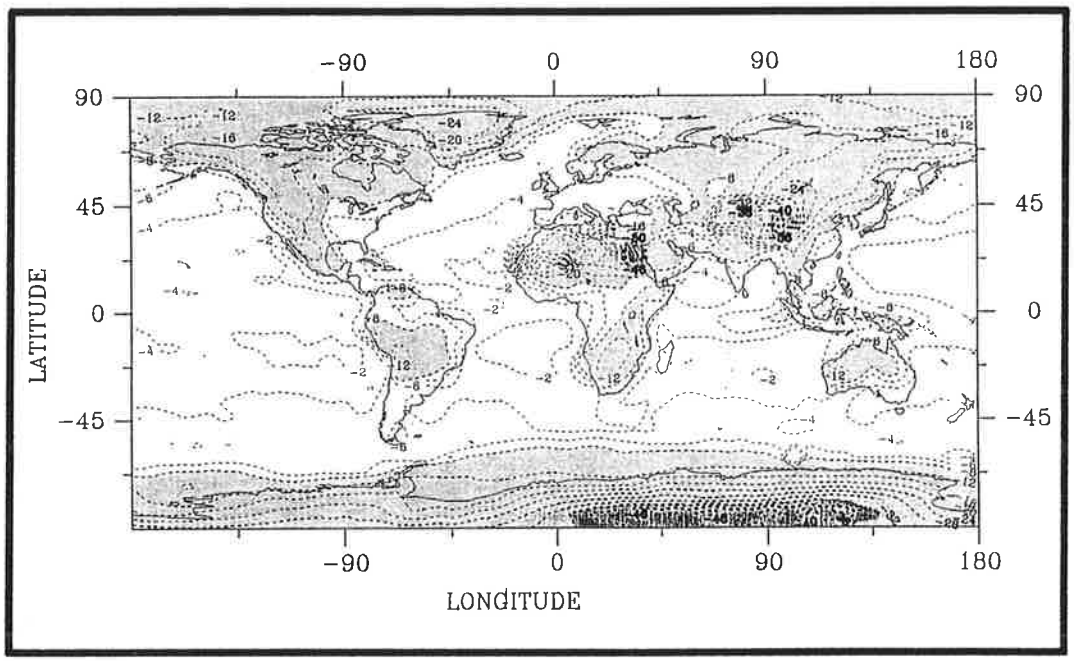

WATER TRACERS IN THE GENERAL CIRCULATION MODEL ECHAM

von

GEORG HOFFMANN • MARTIN HEIMANN

Hamburg, August 1993

AUTHORS:

Georg Hoffmann
Martin Heimann

Max-Planck-Institut
für Meteorologie

MAX-PLANCK-INSTITUT
FÜR METEOROLOGIE
BUNDESSTRASSE 55
D-20146 Hamburg
F.R. GERMANY

Tel.: +49-(0)40-4 11 73-0
Telex: 211092 mpime d
Telemail: MPI.METEOROLOGY
Telefax: +49-(0)40-4 11 73-298

REPb 110

Water tracers in the General Circulation Model ECHAM

1 Abstract

We have installed a water tracer model into the ECHAM General Circulation Model (GCM) parameterizing all fractionation processes of the stable water isotopes ($^1H_2\,^{18}O$ and $^1H^2H\,^{16}O$). A five year simulation was performed under present day conditions. We focus on the applicability of such a water tracer model to obtain informations about the quality of the hydrological cycle of the GCM. The analysis of the simulated $^1H_2\,^{18}O$ composition of the precipitation indicates too weak fractionated precipitation over the Antartic and Greenland ice sheets and too strong fractionated precipitation over large areas of the tropical and subtropical land masses. We can show that these deficiencies are connected with problems of model quantities such as the precipitation and the resolution of the orography. The linear relationship between temperature and the $\delta\,^{18}O$ value, i.e. the Dansgaard slope , is reproduced quite well in the model. The slope is slighly too flat and the strong correlation between temperature and $\delta\,^{18}O$ vanishes at very low temperatures compared to the observations.

2 Introduction

The water isotopes $^1H_2\,^{18}O$ and $^1H^2H\,^{16}O$ belong to the most interesting tracers in climate research. The isotopic water molecules pervade the whole hydrological cycle and undergo fractionation during any evaporation and condensation process. The enrichment of the liquid (or solid) phase relative to the vapour phase depends on temperature, amount of precipitation, relative humidity and many other physical parameters. The relationship between water tracers and climate parameters has been investigated by empirical and theoretical studies [14][9]. Such studies are usually based on simple Rayleigh precipitation models, and the calculated $\delta\,^{18}O$ mainly reflects the temperature difference between the sites of evaporation and precipitation.

Recently, isotopically different water tracers have been used to test the hydrological cycle of General Circulation Models (GCM's) [5][6]. Fractionation processes take place whenever evaporation and condensation occurs. Therefore modelling of water tracers is a good independent test of the hydrological cycle of a GCM, which is probably the most critical process of a climate model. For instance, water tracer concentrations transport information on the location and on how precipition is produced in the model. The isotope content of the precipitation is sensitive to many different parameters and circumstances. Firstly, it is sensitive to the height where condensation has been taken place because of the strong vertical gradient of the isotopic vapour content. Secondly, it is sensitive to the amount of precipitation by influencing in a feedback mechanism the vapour of which the new precipitation will be generated later. Thirdly, it is sensitive to the kind of precipitation by which it has been produced, e.g. big rain drops which are typical for deep convective clouds do not equilibrate completely with its surrounding. Therefore the isotopic composition

ISSN 0937–1060

of the precipitation is a kind of integral property of the atmospheric model.
The model results can be compared with global I.A.E.A. measurements consisting of monthly means of isotope concentration in rain and snow on a fairly dense, worldwide station network spanning more than twenty years. It should also be possible to reproduce with the model results certain empirical relations discovered by Dansgaard [14]; in particular the temperature effect (a linear relation between the surface temperature and the $\delta\,^{18}O$ value) is an important diagnostic feature of the hydrological cycle. For this reason we have implemented water tracers in the ECHAM model by parameterizing all the fractionation and transport processes. Here we describe the results of simulations with the ECHAM model which is the Hamburg version of the GCM of the European Centre for Medium-Range Weather Forecasts (ECMWF) [8]. It is a spectral GCM, which explicitly resolves waves up to zonal wavenumber 21 in the version employed in the present study (T21). The nonlinear terms are calculated on a 64*32 Gaussian grid corresponding to a horizontal resolution of about $5.6° * 5.6°$. The present model version has 19 levels in the vertical dimension defined on hybrid surfaces.

3 The water tracer model

GLOMAC is a tracer transport module which has been embedded in the ECHAM. GLOMAC uses a semi-lagrangian advection scheme for tracer transport [10] and calculates scavenging processes in the clouds. The model has been tested using the atmospheric tracers Lead–210 , Beryllium–7 , Radon–222 and the halocarbon F11 (for details see [11],[4]).
We have modified this model by implementing water tracers which requires the specification of the various fractionation processes between the isotopes. There exist five important parts in the ECHAM model which describe the transport and storage of water (liquid and vapour) – and therefore the water tracers:

1. Adiabatic transport.
2. Turbulent vertical diffusion including evaporation at the surface.
3. Vegetation and soil processes.
4. Large scale condensation.
5. Convective condensation.

1 The adiabatic transport of moisture and of the tracers in the model is computed by a semi-lagrangian scheme. This part was adapted from the GLOMAC nodule.

2 The vertical diffusion equation is solved in the same way for water tracers as for moisture. Four different evaporation fluxes are specified over land: (1) from snow covered soils, (2) from skin water reservoirs and from ground water (either from (3) bare soils or from (4) vegetated areas). These fluxes are expressed as

$$J_{q_x} = \rho C_h C_x |\underline{u}| (q^* - q_{sat}(T_s, p_s)) \qquad (1)$$

Here C_h is the transfer coefficient for moisture , C_x is the fractional area index of the specified surface water pool (1–4), q^* is the specific moisture of the lowest model level and q_{sat} is the saturation specific humidity. The water tracer flux over land J_{xCont} is computed simply by multiplying this moisture flux J_{q_x} with the isotopic ratio of the corresponding surface water pool X_{WP}.

$$J_{xCont} = X_{WP} * J_{q_x} \tag{2}$$

We modify the water tracer flux over ocean surfaces J_{xOce} by using a different saturation value x_{sat}

$$\begin{aligned} J_{xOce} &= \rho C_h |\underline{u}| k (x^* - x_{sat}) && (3) \\ x_{sat}(T_s, p_s) &= q_{sat}(T_s, p_s) * \alpha^{-1}(T) * R_{ocean} && (4) \end{aligned}$$

Here x^* is the tracer mixing ratio in the lowest model level, α the fractionation factor, R_{ocean} the mean oceanic isotope concentration, and q_{sat} the saturation mixing ratio of moisture. We consider the isotopic inequilibrium due to kinetic effects of the ocean surface with the air just above during evaporation by a factor k [7] which depends on the wind velocity.

3 The four different surface water pools over land are balanced similar to water. Runoff, infiltration and drainage are taken into account without any fractionation process (the enrichment of heavy isotopes in vegetation does not seem to be important [6]) .

4 The "large scale condensation" part of the model corresponds to the large, non–convective storm fronts. The model resolves some internal cloud processes such as condensation of vapour into cloud liquid water and ice, autoconversion of droplets into rain and reevaporation of falling rain. Some of these processes are quite slow relative to the residence time of the tracer. Complete isotopic equilibration is therefore assumed for the isotopic water tracer according to the formula (closed system):

$$\frac{x_{cond}}{q_{cond}} = \alpha(T)\frac{x}{q} \tag{5}$$

Here x and x_{cond} are the mixing ratios of the isotopes in the vapour and condensed phase, respectively, q and q_{cond} the corresponding mixing ratios of moisture. Cloud liquid water tracers, which also equilibrate with the surrounding vapour, are implemented analogously to the moisture as a prognostic variable. Solid isotope condensate is formed exclusively below $-40°$C and in a mixture with liquid between $0°$C and $-40°$C. However, since the residence time of solid condensate is much shorter a Rayleigh (or open) system is assumed according to

$$\frac{dx_{cond}}{dq_{cond}} = \alpha(T)\frac{x}{q} \tag{6}$$

According to this formulation only the newly formed solid condensate which is extracted immediately from the system is in equilibrium with vapour.

5 The convective precipitation is parameterized by a mass flux scheme which has been implemented in ECHAM. Such a parameterization distinguishes among three types of clouds depending on the boundary conditions: deep penetrative, shallow and midlevel convection. The newly formed condensate is calculated as in the stratiform case (closed system for liquid, open system for solid condensate). However, since convectively formed drops are significantly bigger, only 50% of these drops are assumed to reach isotopic equilibrium with the surrounding vapour. Additionaly, these big raindrops undergo a kinetic fractionation below the cloud base. This is taken into account by a modified effective fractionation factor.

4 Discussion of the results

A five year run of the water tracer model with oxygen-18 and deuterium has been performed at T21 resolution. We have initialized the integration at January 1st of Year 8 of a control run with the ECHAM model. The atmospheric tracer concentration was initialized with a constant value. The initial concentration in the different surface pools was calculated according to the Dansgaard slope relationship ($\delta^{18}O = 0.69$ t -13.6 ‰) in order to facilitate a faster equilibration. Atmospheric concentrations, surface pools and evaporation fluxes reached equlibrium after a spin-up time of about three months.

4.1 Mean annual $\delta^{18}O$ in precipitation

Figure 1 shows the observed annual mean $\delta^{18}O$ in precipitation. In order to obtain global coverage the $\delta^{18}O$ -values had to be interpolated from the I.A.E.A.- network onto the model grid. Measurements of the isotope concentrations of snow cores in the Antarctic and in Greenland were added [15] [2] [13] [1]. The results of the last four years of the run were averaged. Figure 2 shows the corresponding model results. The most important characteristics are the following:

1 The general isotope ratio pattern, parallel to the annual mean temperatures (i.e. a latitudinal structure) is reproduced. The precipitation over the tropical oceans between 30° N and 30°S shows also the expected isotope ratio between - 2 ‰and -4 ‰.

2 The precipitation over the ice sheets of Greenland and Antarctic is simulated isotopically too heavy. The precipitation which is most strongly fractionated over these areas, deviates by nearly 6 ‰from the observed maxima of -32 ‰(Greenland) and -55 ‰(Antarctic) respectively. In particular, the extension of the area with the isotopically lightest rain (< -36 ‰) over the east antarctic ice sheet is much too small. This holds although the computed temperature in this region is colder than the observed ones (up to 6°C), from which one would expect even stronger fractionation. The reason for this model deficiency may be due to the poor horizontal resolution (Antarctica is represented by two gridpoints in meridional direction only). This will be investigated with a forthcomming run with higher resolution (T42).

3 North Africa shows completely wrong concentrations which are caused by numerical problems. In order to calculate the isotopic concentrations in these regions, very low precipitation values must be divided by the corresponding isotope values, which are also very small.

4 The simulated strong isotope signal over northern India is caused by the Himalayas. This "altitude effect" is also observed near the Rocky Mountains and Andes. If a vapour parcel is lifted, the subsequent precipitation events generate more and more isotopically lighter rain because of the preceding depletion of heavier isotopes in vapour by the increased cooling of the air. This effect does not show up in the observations (Fig.1) since there are no stations near the Himalayas in the I.A.E.A. network.

5 Four further regions show false isotope concentrations: The "cold signature" of strongly fractionated rain extends too far south into Central America; the Amazone basin, southern Africa and western Australia deviate by about -6 ‰from the observed values, lying between -2 and -6 ‰. Deficiencies of the model in temperature, precipitation and in the representation of the orography may explain these problems. In order to get a overview of the quality of these three quantities, we have computed the δ^{18}O value using mean annual temperature (T in °C), annual precipitation (P in m year^{-1}) and altitude (H in m) from the model according to the formula:

$$\delta^{18}O = (0.576T - 0.0114T^2 - 1.35P + 4.47P^2 - 0.147\sqrt{H} - 9.80) * 10^{-3} \quad (7)$$

This formula was obtained by a regression between observed δ^{18}O -values and the corresponding T, P and H [3] . We obtain a similar error pattern by comparing Fig.3 with the measurements (Fig.1): Southern United States/Mexico, the Amazon basin, southern Africa and – less pronounced – western Australia show deviations of nearly -4 ‰up to -8 ‰in the δ^{18}O due to errors in T, P and H alone. We conclude therefore that the differences between model results and observations of the isotope ratio in precipitation is caused rather by model quantities such as precipitation and altitude than by the parameterization of the fractionation processes.
In summary, the land-sea contrast in δ^{18}O seems to be systematically overestimated by the model which indicates additional problems in the parameterization of either surface processes or water tracers.

4.2 Seasonal cycle of δ^{18}O

A comparison of the seasonal cycles of isotope ratios, temperature and precipitation at three different stations is shown in Fig.4. They represent three different cases: 1) The model fits the δ^{18}O data, and simulated temperature and precipitation agree also quite well with the observations. 2) The model does not fit the δ^{18}O data, but the model deficiencies in T and P give us a hint why. 3) The model does not fit the data for unknown reasons.
Case 1 applies to station Chicago. It is remarkable that the big seasonal difference of about -12 ‰ is reproduced at this inland station.
Case 2 applies to the station Truk. Easter Caroline Islands at 7° N and 152° E in

the western Pacific. The deviations of the simulated $\delta^{18}O$ from the observations are significant from July to October which corresponds to the period of largest errors in precipitation. In this region, the $\delta^{18}O$ variations are dominated by precipitation (over 20°C the relation between $\delta^{18}O$ and temperature breaks down and the amount effect dominates). The error of about 220 mm month^{-1} in the predicted precipitation during this period explains the $\delta^{18}O$ error of about 2.5 ‰. It is difficult to reproduce in a GCM the detailed structure of the intertropical convergence zone, because this structure is highly variable. To get a better statistic of the precipitation in this region, we have to integrate the model over a longer period (at least ten years).
The station in Vienna represents case 3. Although the model predicted seasonal cycles of T and P indicate too marine conditions for this mideuropean station, i.e. a seasonal temperature difference of only 14°C instead of 20°C and a much too wet climate all year round, this can not explain the complete lack of seasonality in the simulated $\delta^{18}O$ - values. Possibly this deficiency is due to a too strong tracer transport from the oceanic sources. This will be investigated by a run with higher resolution which should improve this transport.
Figure 5 shows an alternative approach to obtain a overview on a global scale. In order to reproduce the Dansgaard slope we have plotted the annual mean $\delta^{18}O$ versus temperature for all model grid points. In the lower temperature range (< 0°C) we find a good correlation (r=0.94) with a slope of 0.54 $\delta^{18}O$ / °C which is too flat relative to the observed value of 0.64 $\delta^{18}O$ / °C (with r=0.96). However, the correlation in the model already weakens at about 0°C, while the observations show a significant correlation up to 15°C. The reason for this discrepancy which is also observed in the LMD - model [12] is not clear.
The amount effect dominates above 15°C and the temperature correlation vanishes (r=0.15 in the observations, r=0.12 in the model with a slope of 0.06 $\delta^{18}O$ / °C in the observations and 0.05 $\delta^{18}O$ / °C in the model).

5 Conclusions and Outlook

We have implemented a water tracer model in the ECHAM climate model using a similar parameterization scheme as employed by Jouzel et al. [6]. The annual mean and the seasonal cycle of $\delta^{18}O$ were analyzed in order to verify the hydrological cycle of ECHAM. The water tracer model fails to reproduce the annual mean $\delta^{18}O$ value over large areas of the tropical and subtropical land masses by about -6 ‰. We have demonstrated that these deficiencies depend partly on model predicted quantities such as temperature, precipitation and orography. Therefore it will be interesting to investigate a run with higher resolution, which might improve at least the precipitation fields and the representation of the orography.
Marine stations show a less pronounced seasonal cycle relative to continental stations which is due to the permanent vapour source guaranteing nearly constant isotopic boundary conditions ($\delta^{18}O \approx 0.$) throughout the year. The isotope concentration of the vapour which determines the isotope content of the precipitation varies therefore only slightly with sea surface temperature. Over the continents, not only the seasonal temperature cycle is stronger, but also reevaporation of isotopically light water from the soil becomes more important when the isotopic vapour is farther

away from its oceanic sources. A too weak seasonal cycle of $\delta^{18}O$ at continental stations like Vienna indicates therefore a too strong marine influence.
In a next step, the analysis of the deuterium excess ($d = \delta D - 8^* \delta^{18}O$) will offer more information about details of the hydrological cycle.
Further we plan to perform some sensitivity studies with the water tracer model to investigate the importance of the different fractionation processes. For instance, the degree of equilibration of falling rain drops with the surrounding vapour (100% for large scale and 50% for convective clouds respectively) is chosen quite arbitrary and can be varied in sensitivity runs. The quality of the simulated hydrological cycle depends crucially on the resolution of the model. Therefore we shall repeat the experiment at T42 resolution.
Furthermore we intend to run the model under paleoclimate boundary conditions thereafter. Such an experiment offers the possibility to compare the model results directly with proxy measurements (i.e. isotope concentrations in paleowaters and ice). In addition we can test the assumption whether the widely used relationship between $\delta^{18}O$ and temperature also holds when reconstructing the climate of the past.

References

[1] Lorius C. Antarctica: Survey of near–surface mean isotopic values. In G. de Q. Robin, editor, *The climate record of the polar ice sheet*, pages 52–56. Cambridge University Press, New York, 1983.

[2] Lorius C. and Merlivat L. Distribution of mean surface stable isotope values in east antarctica; observed changes with depth in a coastal area, isotope and impurities in snow and ice. *IAHS Publ.*, 118:127–137, 1977.

[3] Farquhar G.D., Lloyd J., Taylor J.A., Flanagan L.B., Syvertsen J.P., Hubick K.T., Chin Wong S., and Ehleringer J.R. Vegetation effects on the isotope composition of oxygen in atmospheric CO_2. *Nature*, 363:439–443, 1993.

[4] Feichter J., Brost R. A., and Heimann M. Three-dimensional modeling of the concentration and deposition of ^{210}Pb aerosols. *J. Geophys. Res.*, 96:22447–22460, 1991.

[5] Joussaume J., Sadourny R., and Jouzel J. A general circulation model of water isotope cycles in the atmosphere. *Nature*, 311:24–29, 1984.

[6] Jouzel J., Russell G.L., Suozzo R.J., Koster R.D., White J.W.C., and Broecker W.S. Simulations of the HDO and H_2O^{18} atmospheric cycles using the NASA GISS General Circulation Model: The seasonal cycle for present day conditions. *J. of Geophys. Res.*, 92:14739–14760, 1987.

[7] Merlivat L. and Jouzel J. Global climatic interpretation of the deuterium–oxygen 18 relationship for precipitation. *J. of Geophys. Res.*, 84:5029–5033, 1979.

[8] Modellbetreuungsgruppe. The ECHAM3 atmospheric general circulation model. Technical Report 6, Deutsches Klimarechenzentrum, Bundesstr. 55 D-20146 Hamburg, 1992.

[9] Ciais P. and Jouzel J. Deuterium and oxygen 18 in precipitation: A new isotopic model including mixed cloud processes. submitted to J. Geophys. Res., ??

[10] Rasch P.J. and Williamson D.L. Computational aspects of moisture transport in global models of the atmosphere. *Q. J. R. Meteorol. Soc.*, 116:1071–1090, 1990.

[11] Brost R.A., Feichter J., and Heimann M. Three-dimensional modeling of ^{7}Be in a global climate model. *J. Geophys. Res.*, 96:22423–22445, 1991.

[12] Joussaume S. and Jouzel J. Paleoclimatic tracers: An investigation using an atmospheric general circulation model under ice age conditions, part 2: Water isotopes. *J. Geophys. Res.*, 98:2807–2830, 1993.

[13] Morgan V.I. Antarctic ice sheet surface oxygen isotope values. *J. Glaciol.*, 28:315–323, 1982.

[14] Dansgaard W. Stable isotopes in precipitation. *Tellus*, 16:436–468, 1964.

[15] Dansgaard W., Johnsen S.J., Clausen H.B., and Gundestrup N. Stable isotope glaciology. *Medd.Groenl.*, 197:1–53, 1973.

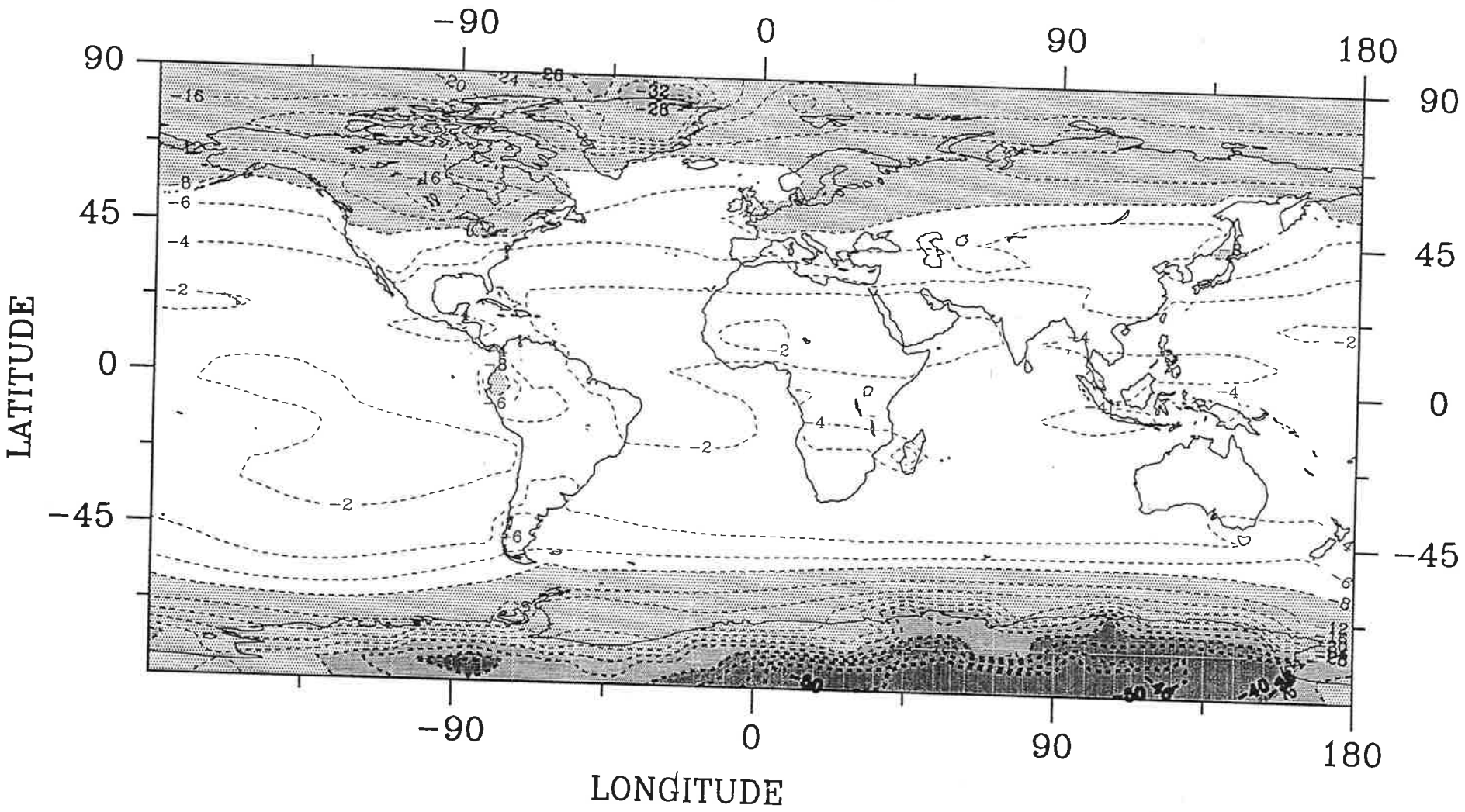

Fig.1: Observed annual mean $\delta^{18}O$ in precipitation. I.A.E.A.-data and additional data in the Antarctic and Greenland interpolated onto a global model grid. Very dark shaded areas correspond to $\delta^{18}O$ values < -36 ‰, dark shaded to < -28 ‰ and light shaded to < -8 ‰.

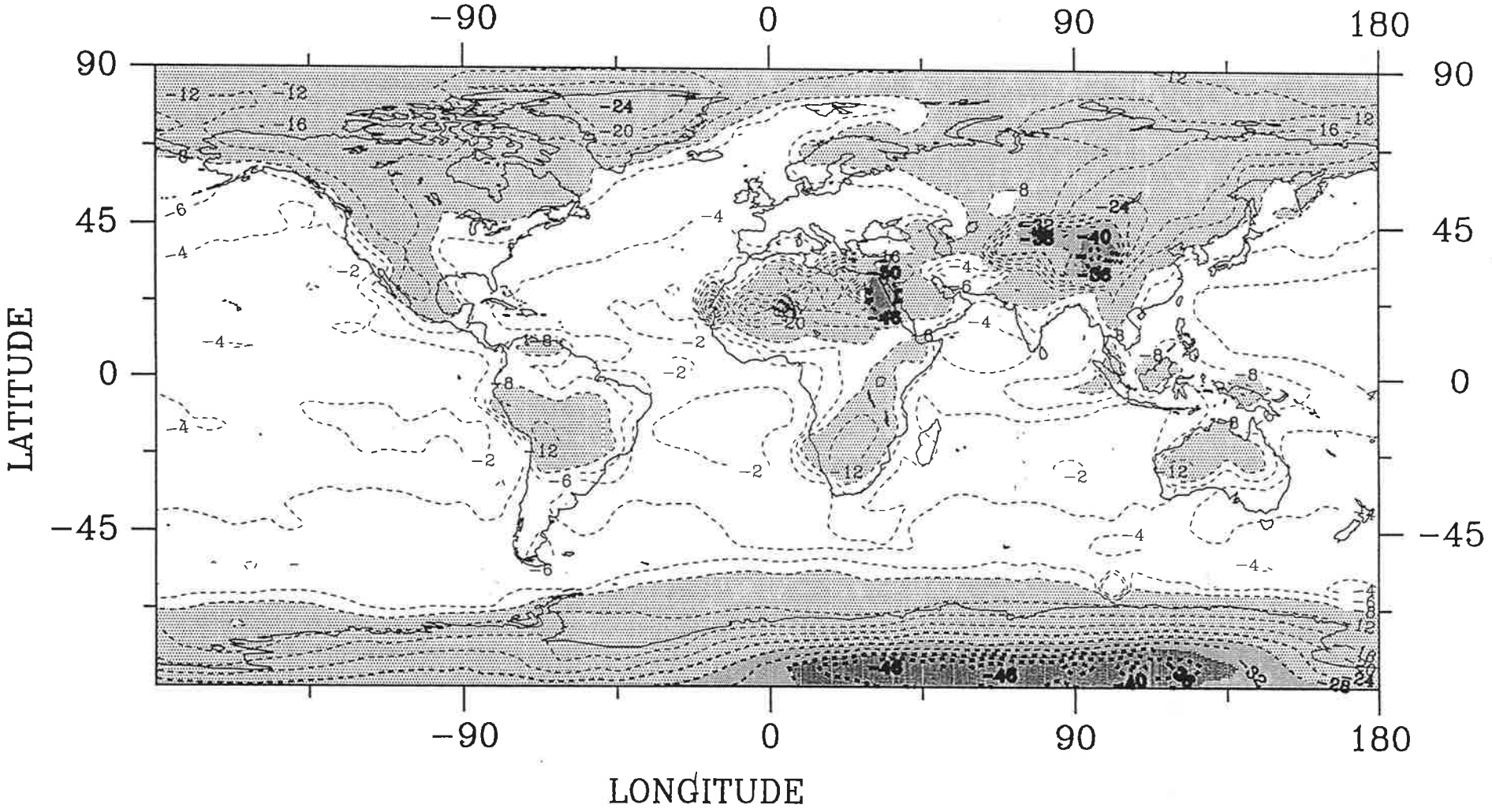

Fig.2: Annual mean $\delta^{18}O$ in precipitation predicted by ECHAM in T21- resolution. Shading as in Fig.1.

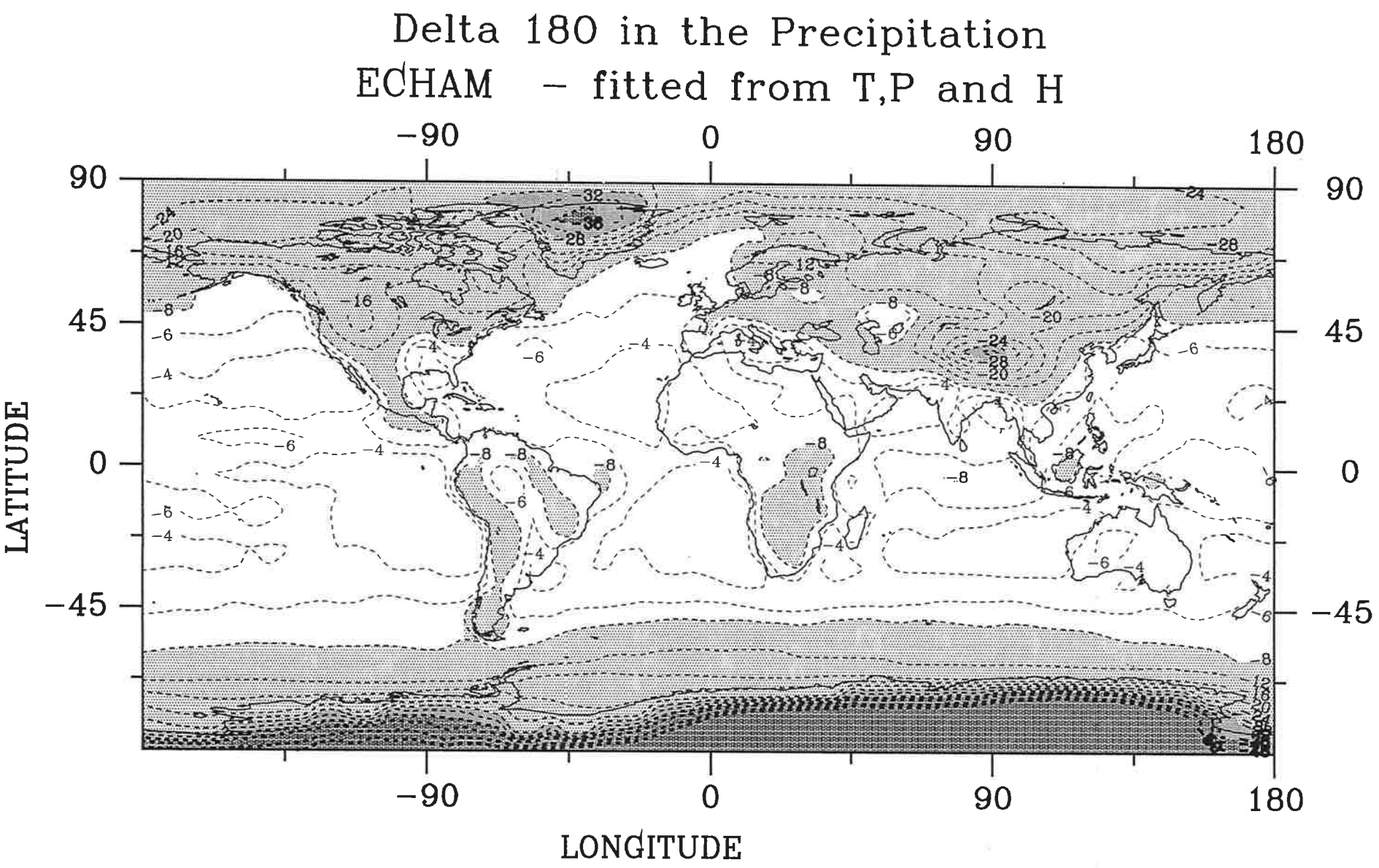

Fig.3: $\delta^{18}O$ in precipitation calculated by the regression formula (7) using annual mean temperature, precipitation and altitude predicted by ECHAM. Shading as in Fig.1

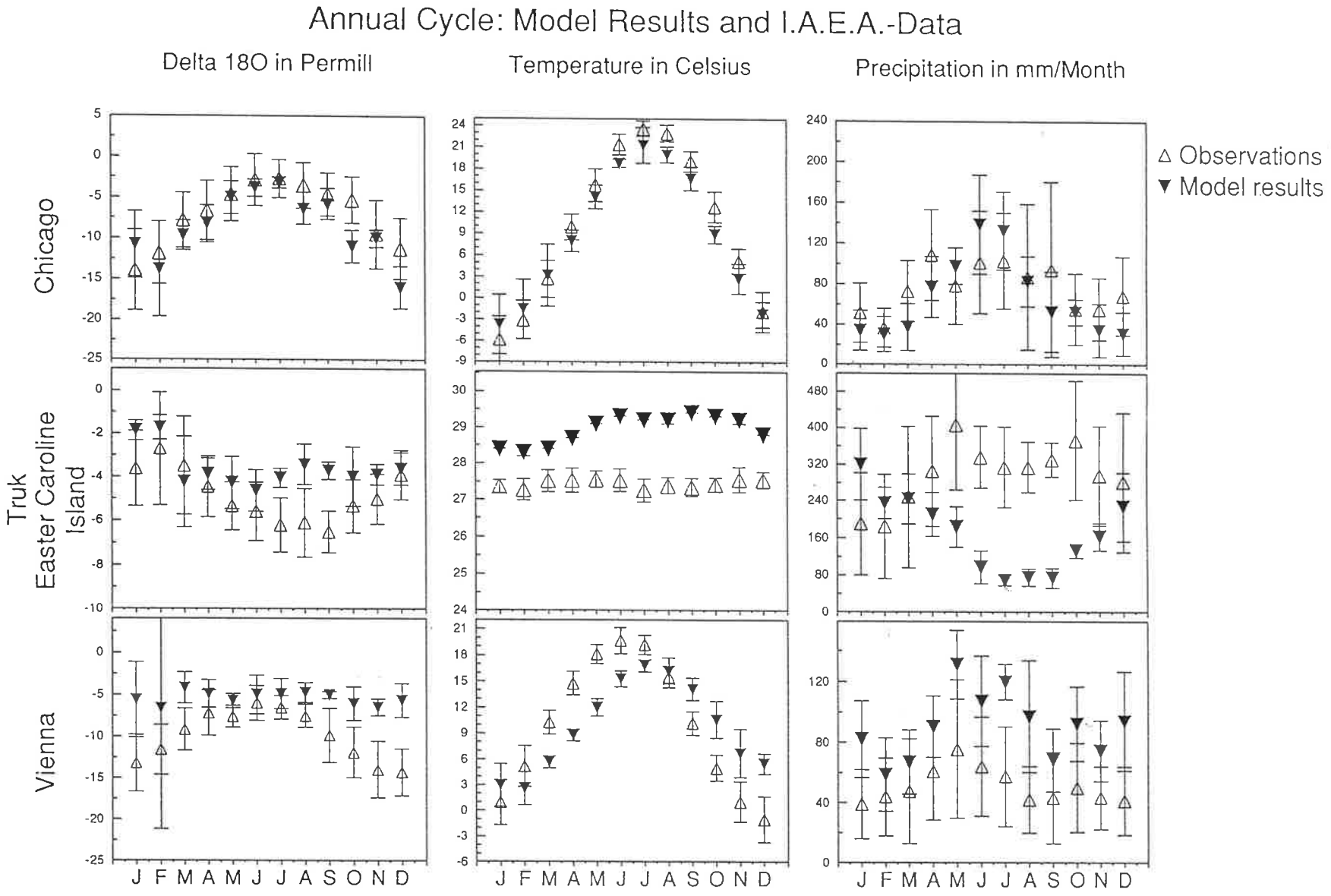

Fig.4: Seasonal cycle of $\delta^{18}O$, temperature and precipitation at three different stations. Observations and model results. Error bars indicate the monthly variation of the four simulated years and of the whole observation period respectively.

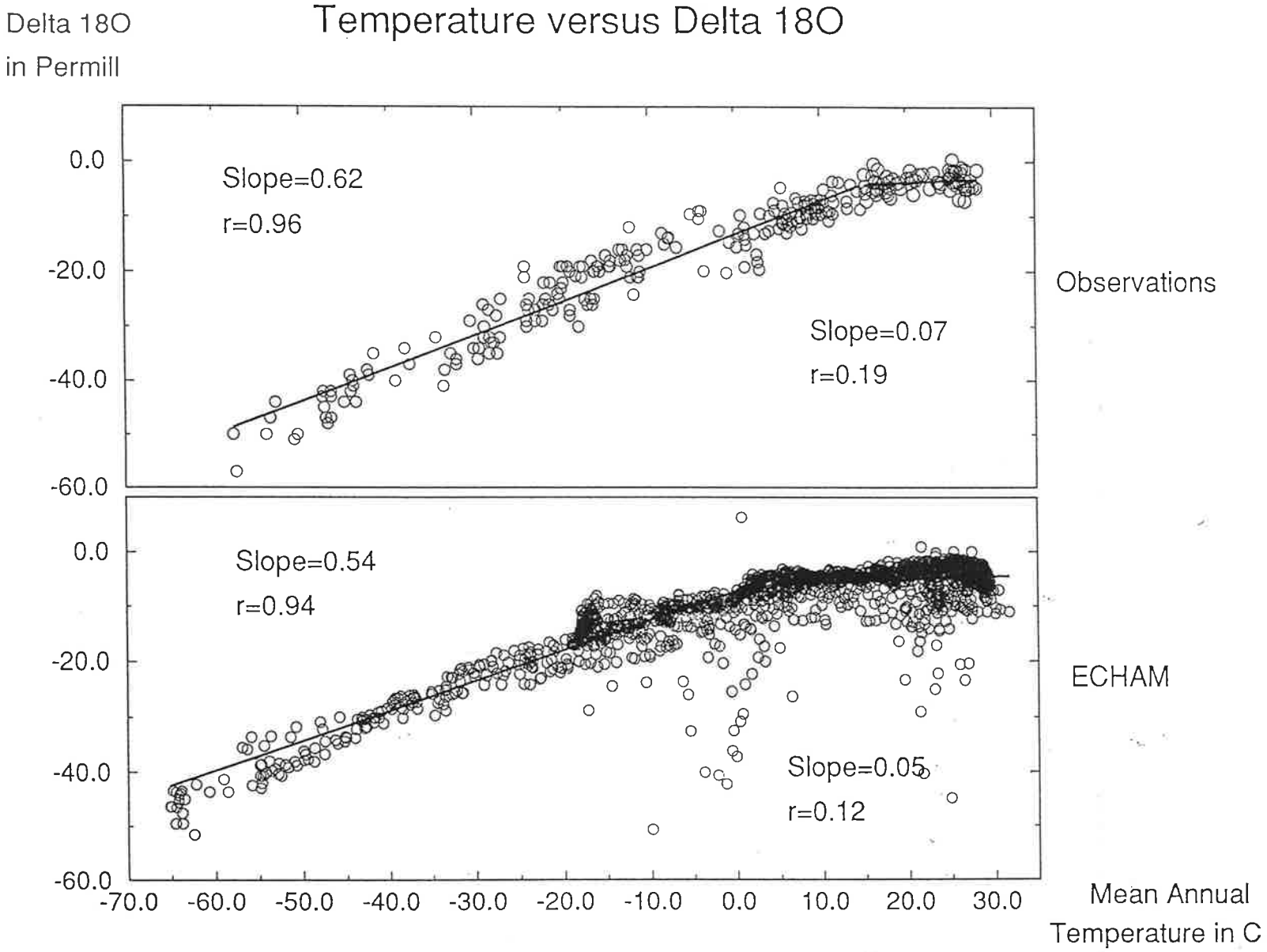

Fig.5: The upper diagram shows the mean annual temperature versus $\delta^{18}O$ at all available stations and the results of a linear regression. The lower diagram shows the same for all model grid points (mean over 4 years).